

A NEW METHOD FOR THE DETECTION OF BRAIN STEM IN TRANSCRANIAL ULTRASOUND IMAGES

Josef Schreiber *, Eduard Sojka *, Lačezar Ličev *, Petra Škňouřilová †, Jan Gaura *

* *Department of Computer Science, † Department of Applied Mathematics*

VŠB - Technical University of Ostrava, 17. listopadu 15/2172

Ostrava - Poruba, Czech Republic

David Školoudík

Neurological clinic, Faculty Hospital in Ostrava-Poruba, 17. listopadu 1790, Ostrava - Poruba, Czech Republic

Keywords: Ultrasound images, brain stem, detection, noise, speckle, Parkinson's disease, object recognition.

Abstract: Transcranial sonography is to date the only method able to detect structural damage of the brain tissue in the Parkinson's disease patients. The problem is that the images provided by this method often suffer from a very poor quality, which makes the final diagnosis strongly dependent on experience of examining medical doctor. Our objective is to create a method that should help to minimize the physician's subjectivity in the final diagnosis and should provide more exact information about the processed ultrasound images. The method itself is divided into two phases. In the first one, we try to locate the position of a minimal window containing the brain stem in the analyzed image. In the second phase, we locate and measure the echogenic substantia nigra area.

1 PARKINSON'S DISEASE

Parkinson's disease (PD) belongs to the neurodegenerative diseases affecting mostly older people. It is a chronic progressive disease that occurs if the nerve cells in a part of the midbrain, called the substantia nigra, die or are impaired. These nerve cells produce dopamine, an important chemical messenger that transmits signals from the substantia nigra to other parts of the brain. These signals allow coordinated movement. If the dopamine-secreting cells in the substantia nigra die, the other movement control centers in the brain become unregulated. Neuroimaging methods are increasingly used as diagnostic tools in patients presenting with parkinsonism. However, brain computed tomography (CT) and magnetic resonance imaging (MRI) examinations are only able to detect other aetiology than PD (Ressner, 2007). This is why these traditional displaying methods like CT and MRI are not considered to be conclusive (Bogdahn, 1998).

In 1995 Becker et al. published a study dealing with the diagnostics of PD using transcranial sonography (Becker, 1995). They showed that increased

echogenicity of substantia nigra is closely associated with PD. Later, their research was followed by other authors (Berg, 1999), (Berg, 2001). They proved that hyperechogenic substantia nigra can be found in more than 91% patients with PD. Nowadays the transcranial sonography is considered to be the best possible diagnostic tool for a detection of structural damage of brain tissue in Parkinson's disease patients. Ultrasonic imaging is based on detecting reflected and scattered waves arising as a response to the emitted wave with various frequencies. In general, the higher the frequency is, the better and more detailed output images can be obtained. Unfortunately, in the case of transcranial sonography, we need to deal with the skull that behaves as a barrier stopping all high-frequency waves. This means that only the low frequency probes (1-4 MHz) may be used. As a consequence of this, transcranial sonography provides images of significantly lower quality (see Figure 1).

The interpretation of ultrasound images is generally a difficult task and the opinion of different medical doctors is generally equivocal. The problem is even more serious in transcranial sonography. Even if the image is carefully evaluated by a physician, there



Figure 1: An example of processed sono image.

is a significant influence of subjectivity. By two different medical doctors, a different diagnosis may be determined from one image. Another problem is a long time treatment when the progress of the disease must be determined from old images and repeating of examination is no longer possible (Školoufík, 2007). That is why there appeared the demand to create a tool that would help physicians to objectivize the diagnosis process. The processing of ultrasound images is widely discussed in literature. Various methods were presented for an image segmentation (Noble, 2006), (Boukerroui, 2003), (Bosch, 2002), noise and speckle reduction (Magnin, 1982), (Rakotomamonjy, 2000), (Kerr, 1986) or image enhancement (Lee, 1980), (Sattar, 1997). However, according to our knowledge, there are no studies dealing with processing the brain-stem transcranial images or with computerized recognition of objects in the substantia nigra area.

Since the image segmentation is strongly dependent on the character of the processed image we need to realize that the usage of classic ultrasound image segmentation methods will be limited. Still, some interesting studies dealing with ultrasound images were published. Ballard et al. (Ballard, 1982) presented region-based segmentation methods such as the region growing where they used the homogeneity of inner regions in the images. Such approach is obviously inappropriate for transcranial images processing since the images contain too much ultrasound speckle. Mishra et al. (Mishra, 2006) presented the active contour method in combine with the genetic algorithms for the endocardial border detection. A slightly different approach was used by Mignotte (Mignotte, 2001). They used a statistical external energy in a discrete active contour for the segmentation of parasternal images. Their work was followed by many optimization efforts, e.g., Heitz (Heitz, 1994). The method provided relatively good results and is recommended for the noisy ultrasound images. Still,

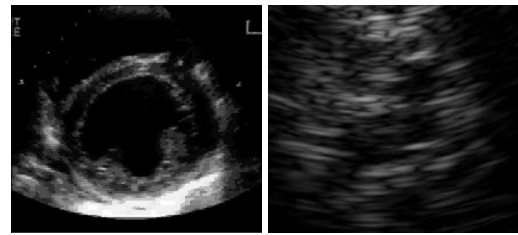


Figure 2: An endocardial (left) and transcranial (right) ultrasound image. The different level of noise is evident.

if we compare the level of noise in the images the method was tested on with transcranial ultrasound images, we see that our analysed images have significantly worse quality.

Another possible method for an ultrasound image segmentation are the level sets, using an adaption of the fast marching method. In 2003, Yan et al. (Yan, 2003) presented the purely edge-based version of this method for the endocardial boundary detection. It was later improved by Lin et al. (Lin, 2003). Their method combined an edge and a region information in a level set approach across spatial scales and it assumes that a boundary is a closed curve. The method is supposed to work well with the images of reasonably good quality. Klinger et al. (Klinger, 1988) presented a study dealing with the echocardiographic images, based on mathematical morphology. As well as the previous method, this one also assumes to work with good quality images. In 1999, Rekeczsky et al. (Rekeczsky, 1999) and Binder et al. (Binder, 1999) came with the artificial neural network method. Binder used a 2-layer backpropagation network to identify a 7×7 pixels region with good results. Unfortunately, we try to locate a region 120×120 pixels large which means a significant growth of input information for the neural network. Even if we decide to use only some important parts of the image to reduce the input, we still have to deal with the possibility that the selected region is strongly covered by ultrasound speckle. Our proposed method is designed to use as much information from analysed image as possible to avoid being misled by the high level of ultrasound noise and speckle.

2 BRAIN STEM LOCALIZATION

The method we have developed for processing the brain-stem transcranial sono images is divided into two phases. In the first phase, we try to locate the position of a minimal window in the processed image containing the brain stem. To do so, we use a modified template matching algorithm. Since every human being is unique, the brain stems may slightly

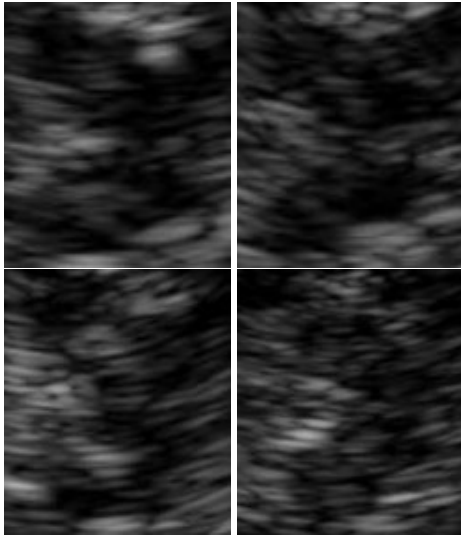


Figure 3: Examples of the images used for the template construction. For need of this paper, the images are displayed with the same size.

differ in shape and size. Moreover, the objects being sought inside the stem may have different position, size, and echogenicity, depending on the disease progress. Therefore, for creating the template of the stem, we choose several images that best represent, according to our opinion, various possible shapes and sizes of the stem. We also consider the seriousness of the disease by choosing images depicting the situation in various stages of the disease progress (from healthy persons to persons with an advanced stage of the disease). The selection of images that are used for the template construction is important in our method. Therefore, the selection of images was widely discussed with medical doctors to best fulfill previously mentioned parameters. Overall, there were 20 selected images used for the template construction. Four examples of these images can be seen in Figure 3.

We construct the template that is used for matching by simple averaging the particular selected images of the brain stem. Firstly, the images are normalized to the same size. In our experimental implementation, we use the size of 120×120 pixels. After normalizing the size, we normalize the images of stem also with respect to the mean value and the variance of brightness. We do so by using the following formula

$$b_n(\mathbf{x}) = ab_o(\mathbf{x}) + c, \quad (1)$$

where $b_n(\mathbf{x})$, $b_o(\mathbf{x})$ stand for the normalized and original brightness, respectively, at a pixel whose position is described by a two-dimensional vector \mathbf{x} , and a and c are constants that must be determined for each particular image. For determining them, the mean value

of brightness, denoted by μ_{bo} , and the variance of brightness, denoted by σ_{bo}^2 , in the original images are needed. Let Ω stand for the set of all pixels in the brain-stem image and let N be the size of this set. We have

$$\mu_{bo} = \frac{1}{N} \sum_{\mathbf{x} \in \Omega} b_o(\mathbf{x}), \quad (2)$$

$$\sigma_{bo}^2 = \frac{1}{N} \sum_{\mathbf{x} \in \Omega} (b_o(\mathbf{x}) - \mu_{bo})^2. \quad (3)$$

In each normalized image, the normalization of brightness aims at achieving a certain required mean value, denoted by μ_{bn} and a required variance of brightness, denoted by σ_{bn}^2 . Simple mathematics yields the following formulas for a and c

$$a = \frac{\sigma_{bn}}{\sigma_{bo}}, \quad c = \mu_{bn} - a\mu_{bo}. \quad (4)$$

The effect of normalization can be seen in Figures 4, 5. In Figure 6, the set of example images from Figure 3 can be seen in normalized form. An example of the template that was obtained by averaging the brain-stem images using Equation 5 is depicted in Figure 7.

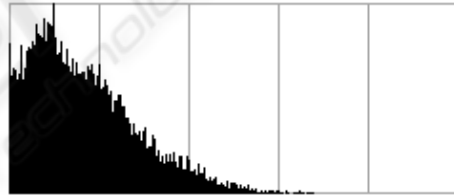


Figure 4: The histogram of original image.

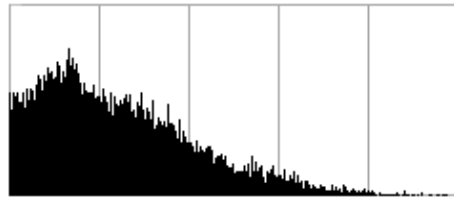


Figure 5: The histogram of normalized image.

In the pattern matching algorithm, we will also use the variance of brightness in particular pixels that can be expressed as follows

$$\mu_b(\mathbf{x}) = \frac{1}{M} \sum_{j=1}^M b_{nj}(\mathbf{x}), \quad (5)$$

$$\sigma_b^2(\mathbf{x}) = \frac{1}{M} \sum_{j=1}^M (b_{nj}(\mathbf{x}) - \mu_b(\mathbf{x}))^2. \quad (6)$$

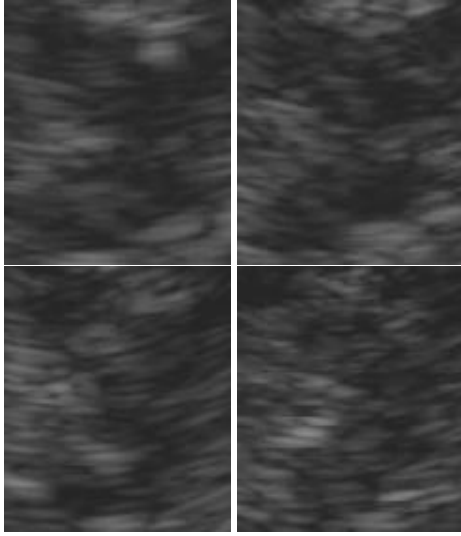


Figure 6: The brain-stem images from Figure 3 after the normalization process.

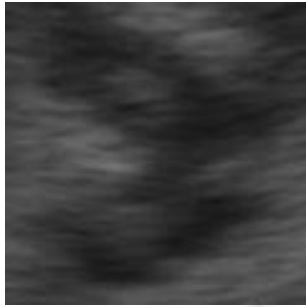


Figure 7: The constructed template.

In the above formulas, M is the number of particular normalized brain-stem images that are used for creating the template; b_{nj} stands for the j -th such image.

In the first step of our method, we try to locate the position of the brain stem. We introduce a possibility, denoted by $\pi(\mathbf{u}_k, \mathbf{x})$, of the event that the template point with the coordinates \mathbf{x} corresponds to the image point with the coordinates $\mathbf{x} + \mathbf{u}_k$ (Sojka, 2006). This possibility may be determined from the difference of brightness

$$\Delta b = b(\mathbf{x} + \mathbf{u}_k) - t(\mathbf{x}), \quad (7)$$

where $b(\mathbf{x} + \mathbf{u}_k)$ is the brightness of the pixel with coordinates $\mathbf{x} + \mathbf{u}_k$ in processed image, and $t(\mathbf{x})$ is the brightness in the corresponding template pixel. Let it be pointed out that \mathbf{u}_k characterizes the template position that is just being processed.

We suppose that the possibility distribution may be described by a certain chosen function φ . Figure 8 shows an example of such a function. For the con-

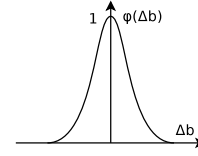


Figure 8: The distribution of possibility φ (we use the Gaussian function).

struction of φ , we use the deviation $\sigma_b(\mathbf{x})$ that was determined in Equation 6.

To obtain the possibility of the event that the image pixel just being processed corresponds to the pixel from the template, we use the following equation

$$\pi(\mathbf{u}_k, \mathbf{x}) = \varphi(b(\mathbf{x} + \mathbf{u}_k) - t(\mathbf{x}), \sigma_b(\mathbf{x})). \quad (8)$$

To characterize the quality of matching at the position \mathbf{u}_k , we introduce the quantity $S(\mathbf{u}_k)$ characterizing the number of pixels, i.e., the "net area" that can successfully be matched to the template. We have

$$S(\mathbf{u}_k) = \sum_{\mathbf{x} \in \Omega} \pi(\mathbf{u}_k, \mathbf{x}), \quad (9)$$

where Ω stands for the set of template pixels.

The final goal is to find the value of \mathbf{u} that maximizes the value of $S(\mathbf{u}_k)$. The value of \mathbf{u} then determines the position of the window that should contain the brain stem (Figure 9).

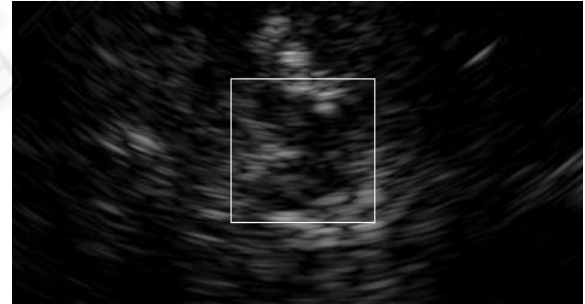


Figure 9: An image with the recognized brain-stem object.

It is obvious that during the brain-stem detection, each processed window from the analyzed image must be normalized in the same way as the images used for the template construction.

3 ANALYSIS OF BRAIN STEM

To obtain the information about the disease progress, we now need to locate and measure the objects inside the brain stem, which is the second step of our



Figure 10: An image with the recognized brain stem and the highlighted objects.

method. In the image, these objects appear as the areas with a higher level of echogenicity inside the substantia nigra area. It is a difficult task to correctly identify these objects because the areas may have insufficient contrast.

We locate the objects in the brain stem as the areas with a higher level of brightness that are found using the region growing method. Homogeneity of brightness is a criterion that is used for growing. After growing, the regions of interest are usually partitioned into several smaller areas (Figure 10). Therefore, morphological closing is carried out after growing to connect the sub-areas together. If it is required by a doctor, the convex hull of the found area may be computed too. The regions that have been found are then checked for the shape and size, which separates the objects of interest in the stem. The numerical characteristics are then computed. For all recognized objects, we determine the number of pixels the objects are composed of, their average brightness, and the location of their gravity centers. Besides computing the characteristics of the objects, they can also be highlighted in the images (Figure 10).

Naturally, there is also a possibility to correct the obtained results manually, if necessary, and remove possible unwanted objects that are considered to be only a noise, ultrasound speckle or possibly even a part that does not belong to the brain stem area.

4 ACHIEVED RESULTS

To test the successfulness of our method in brain stem localization, we used a sample of 170 images in which we tried to locate the correct brain-stem position. The result (the quality of recognition) was classified with the marks between 1 and 3. The mark 1 means that the position was recognized correctly and accurately. The mark 2 means that the position was determined inaccurately but not completely incorrectly. In this case, the position was usually determined with an error up

to 10-15 pixels. The mark 3 means that the method determined an incorrect position. For our set of test images, we obtained the results that are summarized in Table 1.

Table 1: The results of the brain-stem localization achieved by the presented method. The first column determines the quality of recognition. The second one shows the number of images recognized with corresponding quality and the last column displays the overall percentage.

Quality of recognition	Number of images	Results in %
1	129	75,9
2	4	2,3
3	37	21.8

The mark 1 was achieved in nearly 76% of images. This can be considered as a good result since we have to realize that the method must deal with images of various quality. The difference between the good and bad image is shown in Figure 11. In the left image, we can clearly see the shape of the brain stem. For our method, the right image is very difficult to determine the correct brain-stem location.

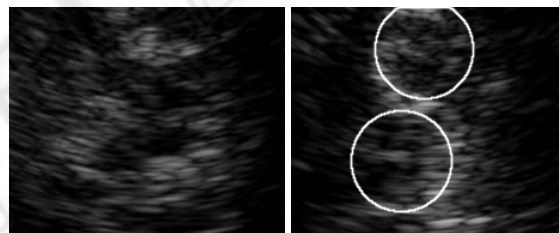


Figure 11: These images illustrate the difference between the good quality and the bad quality images. While in the left image, the shape and position of brain stem is obvious, in the right image, two places with similar shape to the brain stem may be found.

5 CONCLUSIONS

The computer processing of transcranial ultrasound images is a complicated task. Images often suffer from a very poor quality and they often have a high level of noise and speckle. The objects that were recognized are often discontinuous, in worse cases even incomplete. The objects inside the brain stem often have insufficient contrast and they are usually fragmented by ultrasound speckle. Still, the objective evaluation of these images can be very helpful in the Parkinson disease diagnostics and treatment. It can help the medical doctors to determine the correct diagnosis as well as the level of the disease progress.

The exact and objective information about the examination from particular date can especially help in longer time diagnostics when repeating of the examination is no longer possible.

Our method may be divided into two phases. At first, it attempts to correctly identify the position of brain stem in processed image. This phase is crucial in overall diagnostics and this paper focuses mostly on this part. In the second phase, we detect the objects of interest in the brain stem. The detection of existence, shape, size, and echogenicity of these objects is a valuable contribution to the diagnostics of Parkinson's disease.

Achieved results obtained during testing make us believe that the method we have developed for the detection and analysis of the brain stem in transcranial ultrasound images is successful. From the tested images, we obtained good results. In 76% of cases, the position of the brain stem was correctly determined.

ACKNOWLEDGEMENTS

Presented results had been obtained during solving the grant project code T401940412 supported by the Academy of Sciences of the Czech Republic.

REFERENCES

- Ballard, D.H., B. C. (1982). *Computer vision*. Prentice-Hall, Englewood Cliffs, NJ.
- Becker, G., B. U. G. C. e. a. (1995). Transcranial color-coded real-time sonography of intracranial veins. normal values of blood flow velocities and findings in superior sagittal sinus thrombosis. *Journal of Neuroimaging*, 5:87–94.
- Berg, D., B. G. Z. B. T. O. H. E. e. a. (1999). Vulnerability of the nigrostriatal system as detected by transcranial ultrasound. *Neurology*, 53:1026–1031.
- Berg, D., S. C. B. G. (2001). Echogenicity of the substantia nigra in parkinson's disease and its relation to clinical findings. *Journal of Neurology*, 248:684–689.
- Binder, T., S. M. M. D. S. H. B. T. M. G. P. G. (1999). Artificial neural networks and spatial temporal contour linking for automated endocardial contour detection on echocardiograms: A novel approach to determine left ventricular contractile function. 25(7):1069–1076.
- Bogdahn, U., B. G. S. F. (1998). *Echoenhancers and transcranial color duplex sonography*. Blackwell Science, Berlin.
- Bosch, J.G., M. S. L. B. N. F. K. O. S. M. R. J. (2002). Automatic segmentation of echocardiographic sequences by active appearance motion models. 21(11):1374–1383.
- Boukerroui, D., B. D. N. J. B. O. (2003). Segmentation of ultrasound images - multiresolution 2d and 3d algorithm based on global and local statistics. *Pattern Recognition Letters*, 24(4-5):779–790.
- Heitz, F., P. P. B. P. (1994). Multiscale minimization of global energy functions in some visual recovery problems. 59:125–134.
- Kerr, A.T., P. M. F. F. H. J. (1986). Speckle reduction in pulse echo imaging using phase insensitive and phase sensitive signal processing techniques. 8:11–28.
- Klinger, J.W.J., V. C. F. T. A. L. T. (1988). Segmentation of echocardiographic images using mathematical morphology. 35(11):925–934.
- Lee, J. (1980). Digital image enhancement and noise ltering by use of local statistics. *PAMI-2(2)*:165–168.
- Lin, N., Y. W. D. J. (2003). Combinative multi-scale level set framework for echocardiographic image segmentation. 7(4):529–537.
- Magnin, P.A., v. R. O. T. F. (1982). Frequency compounding for speckle contrast reduction in phased array images. *Ultrasonic Imaging*, 4:267–281.
- Mignotte, M., M. J. (2001). A multiscale optimization approach for the dynamic contour-based boundary detection issue. 25(3):265–275.
- Mishra, A., D. P. G. M. K. (2006). A ga based approach for boundary detection of left ventricle with echocardiographic image sequences. 21(11):967–976.
- Noble, J.A., B. D. (2006). Ultrasound image segmentation: A survey. *IEEE Transactions on medical imaging*, 25(8):987–1010.
- Rakotomamonjy, A., D. P. M. P. (2000). Wavelet-based speckle noise reduction in ultrasound b-scan images. 22:73–94.
- Rekeczky, C., T. A. V. Z. R. T. (1999). Cnn-based spatiotemporal nonlinear filtering and endocardial boundary detection in echocardiography. 27(1):171–207.
- Ressner, P., v. D. H. P. K. P. (2007). Hyperechogenicity of the substantia nigra in parkinson's disease. *Journal of Neuroimaging*, 17(Issue 2):164–167.
- Sattar, F., F. L. S. G. L. B. (1997). Image enhancement based on nonlinear multi-scale method. 6:888–895.
- Sojka, E. (2006). A motion estimation method based on possibility theory. In *Proceedings of IEEE ICIP*, pages 1241–1244.
- Školoufík, D., F. T. B. P. L. K. R. P. Z. O. H. P. H. R. K. P. (2007). Reproducibility of sonographic measurement of the substantia nigra. *Ultrasound in Medicine & Biology*, 33(9):1347–1352.
- Yan, J.Y., Z. T. (2003). Applying improved fast marching method to endocardial boundary detection in echocardiographic images. 24(15):2777–2784.